Current Research in Microbial Sciences 3 (2022) 100152

Contents lists available at ScienceDirect

Current Research in Microbial Sciences

journal homepage: www.sciencedirect.com/journal/current-research-in-microbial-sciences

Biological features of TcM: A new *Trypanosoma cruzi* isolate from Argentina classified into TcV lineage☆

Santiago José Martinez [a], Gonzalo Nicolás Nardella [b], Matías Exequiel Rodríguez [c], Cynthia Vanesa Rivero [a], Fernán Agüero [c], Patricia Silvia Romano [a,d,*]

[a] *Laboratorio de Biología de Trypanosoma cruzi y la célula hospedadora. Instituto de Histología y Embriología, Universidad Nacional de Cuyo (IHEM-CONICET-UNCUYO), Mendoza, Argentina*
[b] *Facultad de Farmacia y Bioquímica. Universidad Juan A. Maza. Mendoza, Argentina*
[c] *Instituto de Investigaciones Biotecnológicas, Universidad Nacional de San Martín (IIB-CONICET-UNSAM), Buenos Aires, Argentina*
[d] *Facultad de Ciencias Médicas. Universidad Nacional de Cuyo (FCM-UNCUYO), Mendoza, Argentina*

ARTICLE INFO

Keywords:
Trypanosoma cruzi
DTUs
Tissue tropism
Chronic strain
Drug susceptibility

ABSTRACT

Trypanosoma cruzi, the etiologic agent of Chagas disease (CD) presents a wide genetic and phenotypic diversity that is classified into seven lineages or discrete typing units (DTU: TcI to TcVI and Tcbat). Although isolates and strains that belong to a particular group can share some attributes, such as geographic distribution, others like growth rate, cell tropism, and response to treatment can be highly variable. In addition, studies that test new trypanocidal drugs are frequently conducted on *T. cruzi* strains maintained for a long time in axenic culture, resulting in changes in parasite virulence and other important features. This work aimed to isolate and characterize a new *T. cruzi* strain from a chronic Chagas disease patient. The behavior of this isolate was studied by using standard *in vitro* assays and *in vivo* mice infection tests and compared with the *T. cruzi* Y strain (TcY), broadly used in research laboratories worldwide. Data showed that TcM behaves as a slow-growing strain *in vitro* that develops chronic infections in mice and displays high tropism to muscular tissues, in accordance with its clinical performance. In contrast, the Y strain behaved as an acute strain that can infect different types of cells and tissues. Interestingly, TcM, which belongs to DTU TcV, is more susceptible to benznidazole than TcY, a TcII strain considered moderately resistant to this drug. These differential properties contribute to the characterization of a TcV strain, one of the main lineages in the southern countries of South America, and open the possibility to introduce changes that improve the management of Chagas patients in the future

1. Introduction

Trypanosoma cruzi is the etiologic agent of Chagas disease (CD), a neglected tropical disease highly disseminated in the world. Between 6 and 7 million people are infected with *T. cruzi*, mostly in Latin America, where it is endemic (Pérez-Molina and Molina, 2018). *T. cruzi* is a protozoan parasite with a complex biological cycle alternating between insects of the *Reduviidae* family, also called kissing bugs, and mammalian hosts, vectors and reservoirs of CD, respectively. The *T. cruzi* life cycle consists of four stages of development, starting with the epimastigote, the replicative extracellular form of this parasite, which develops in the midgut digestive system of blood-sucking insects. The next form is the infective non-replicative metacyclic trypomastigote (MT), which occurs at the end of the digestive system of insects. When the insect feeds on a mammal, MTs escape through the feces and can enter either through the same laceration produced by the insect or through the mucosa near the bite. MTs infect cells at this place and differentiate into amastigotes, the intracellular replicative form of *T. cruzi*. Amastigotes replicate several times in the host cell cytoplasm and further differentiate into blood trypomastigotes (BTs), which lyse

☆ SJM, GNN, MER and CVR made the experiments. SJM made the figures, and performed the statistical analysis. SJM, FA and PSR contributed to design the experiments. SJM, FA and PR wrote the first draft of the manuscript. SJM and PSR wrote the revised version of the manuscript and editing the figures. All authors contributed to the article and approved the submitted version.

* Corresponding author at: Instituto de Histología y Embriología, Universidad Nacional de Cuyo (IHEM-CONICET-UNCUYO), Casilla de Correo 56, Centro Universitario, Parque General San Martín, (5500) Mendoza, Argentina
E-mail address: promano@fcm.uncu.edu.ar (P.S. Romano).

https://doi.org/10.1016/j.crmicr.2022.100152

Available online 30 June 2022

host cells and infect new cells in the same place or reach the bloodstream to infect other tissues. In the blood, parasites can be transmitted to another kissing-bug, completing the cycle by differentiation of BT to epimastigotes (Tyler and Engman, 2001; Osorio et al., 2012; CDC - Chagas Disease - Biology [Internet]., 2020). The passage of MT to mammals by the bite of triatomine insects, known as vectorial transmission, is produced in endemic countries by the presence of insects in these places. Other routes of infection include blood transfusion and organ transplant, due to the presence of parasites in the blood of donors, the ingestion of contaminated food (digestive route), and the vertical transmission from an infected mother to child during pregnancy, which is the most important form of transmission nowadays mainly in non-endemic countries (Pérez-Molina and Molina, 2018).

Clinically, CD comprises two phases, an acute infection with unspecific symptoms followed by a chronic infection. Most patients remain asymptomatic for decades; however, about 30% of infected individuals develop irreversible cardiomyopathy and 10% digestive or mixed manifestations, which cause approximately 12,000 deaths per year (https://www.who.int/chagas/epidemiology/en/) (Chagas disease - PAHO/WHO | Pan American Health Organization., 2020; Nunes et al., 2013; Andrade et al., 1999; Vago et al., 2000; Lewinsohn, 1981). It is not completely understood why some patients develop cardiac pathology whereas others develop digestive or mixed manifestations. However, recent evidence has shown that tissue damage is a direct consequence of *T. cruzi* presence, which elicits a chronic inflammatory response. Hence, the current consensus is that the balance between persistence of infection and host immune response is crucial for the establishment and progression of pathology (Pérez-Molina and Molina, 2018). In this scenario, the occurrence of parasite strains with different tissue preference or invasion efficiency could represent an additional factor underlying the development of different clinical manifestations (Meymandi et al., 2017; CDC - Chagas Disease - Epidemiology and Risk Factors [Internet]., 2020).

Since its discovery by the Brazilian physician Carlos Chagas in 1909 (Lewinsohn, 1981), CD has been the focus of study in different scientific disciplines, from molecular to epidemiological sciences. The genotypic and phenotypic diversity of *T. cruzi,* its complex life-cycle, and multiple routes of transmission, in addition to the clinical performance of the infection in humans, have turned CD into a complex illness that can cause more deaths than currently registered. It has become a health problem in many countries; in developing countries with scarce health resources as well as in rich countries due to the unawareness of this disease in the past and the persistent lack of effective treatments for the chronic stage (Chagas disease - PAHO/WHO | Pan American Health Organization., 2020; Meymandi et al., 2017; CDC - Chagas Disease - Epidemiology and Risk Factors [Internet]., 2020).

The nitroderivatives Benznidazole (BNZ) and Nifurtimox (NTX) discovered ~50 years ago are the first line of drugs for CD treatment. These are effective in the acute phase, congenital infection, and in children with chronic infections (age below 12 years). However, they are less effective in chronic infection in adults (Coura and De Castro, 2002; Morilla et al., 2004; Velazquez et al., 2015). Trypanocidal therapy in patients with established Chagas cardiomyopathy does not significantly reduce cardiac clinical deterioration and serious side effects occur more frequently in elderly patients (Viotti et al., 2009). Another weakness of the current treatment is the different susceptibility to these drugs displayed by several *T. cruzi* isolates and strains. It has been shown that some strains of *T. cruzi* display more resistance than others to the treatment with BNZ (LP Quebrada Palacio et al., 2018; Medina et al., 2018; MCO Campos et al., 2014). It is noteworthy that, since BNZ discovery in 1970, no new drug has been approved for CD treatment, a fact that can be influenced by the high variability of *T. cruzi.*

As mentioned above, *T. cruzi* displays a wide genetic and phenotypic diversity. A new consensus classified the *T. cruzi* species into seven major lineages, called Discrete Typing Units (DTUs), from TcI to TcVI and Tcbat (Zingales et al., 2009; Zingales et al., 2012; Marcili et al., 2009). Different molecular approaches can be used to classify new isolates and strains into these DTUs (Cura et al., 2015; Cosentino and Agüero, 2012). Interestingly, these lineages exhibit geographical distribution patterns, likely correlated at least in part with transmission through different species of the Reduviidae group. While TcI prevails throughout the American continent, other DTUs are more prevalent in South America, especially in Brazil, where TcII occupies the second most frequent lineage. In contrast, the hybrid lineages TcV and TcVI predominate in the domestic transmission cycles in Argentina (Paula et al., 2018; MAFFEY et al., 2012). Some biological features have also been associated with different DTUs. Attributes, such as the presence of a lineage in domestic or sylvatic cycles and higher metacyclogenesis capacity, were found more frequently in some DTUs than in others (Abegg et al., 2017). Yet, other authors found higher genotypic and phenotypic diversity in strains and isolates within the same lineage (LP Quebrada Palacio et al., 2018; Virreira et al., 2006; Macchiaverna et al., 2018). Another source of variability involves the strains artificially maintained in laboratories for several years, contributing to the loss of their virulence and other properties (Cortez et al., 2012; AF Casassa et al., 2019).

The aims of this work were to obtain a clinical isolate of *T, cruzi* and study its biological properties; virulence, cellular and tissue affinity, development of acute or chronic infections, and drug susceptibility in comparison with *T. cruzi* Y, a laboratory-maintained strain from DTU-II. Data showed that the TcM isolate, obtained from a chronic patient living in Mendoza city (Argentina), belongs to *T. cruzi* DTU TcV and displays a different biological behavior from that of the Y strain. Given the high level of variability exhibited by *T. cruzi,* these properties can be used as a tool to characterize the biology of each particular isolate, predict the outcome of infection, and improve the management of CD in the infected patient (Paula et al., 2018).

2. Materials and methods

2.1. Ethical statement

Two independent Ethical Committees approved this study; the Diego Paroissien Hospital Bioethics Committee and the Central Hospital Investigation Committee (Mendoza-Argentina). The study fulfilled all the criteria required by the Medical Code of Ethics and the Helsinki II statement, required by both committees. This project was also approved by the Departamento de Investigación, Ciencia y Técnica (Dicyt), Ministerio de Salud, Desarrollo social y Deportes del Gobierno de Mendoza.

Animal-based experiments were specifically reviewed and approved by the Comité Institucional para el Cuidado y Uso de Animales de Laboratorio (CICUAL). All animals were purchased from Jackson Laboratory and maintained under Specific Pathogen Free conditions (SPF) and 12 h dark/light cycle at a temperature of 22+3 °C with access to sterilized water and food *ad libitum.*

2.2. T. cruzi isolation

To isolate *T. cruzi* trypomastigotes from human samples, our laboratory established collaboration with the Instituto Coordinador de Ablación e Implante de Mendoza (INCAIMEN) and with the Diego Paroissien Hospital, both from Mendoza, Argentina. Upon detection of positive *T. cruzi* parasitemia, written informed consent was obtained from patients before blood sample extraction. Between 5 and 10 mL of blood was obtained by venipuncture under aseptic conditions using heparin as anticoagulant. The blood extracted from the infected patient was placed on a fresh culture of Vero C-76 and H9c2 cells in T25 flasks or 6 well plates (Biofill®). They were cultivated at 37 °C in an atmosphere of 95% O_2 and 5% CO_2 for up to 5 days to achieve trypomastigote infection. After washing with PBS (Phosphate Buffered Saline) (Gibco®), fresh media were added and cultures were maintained for several days until free trypomastigotes were observed in the media. When enough parasites were available for expansion of the cultures, samples

containing at least 10^6 parasites/mL were taken for cryopreservation. Trypomastigotes were centrifuged at 5000 *g* for 10 min and pellets were suspended in a freezing mix of 90% FBS (Fetal Bovine Serum) and 10% DMSO (Dimethyl Sulfoxide). Samples were divided into vials and frozen in a Styrofoam box overnight (ON) at –80 °C before passage to liquid N_2. The remaining parasites were used for the experimental procedures. The new *T. cruzi* isolate was named TcM (*M* = Mendoza, the city where the patient lives), and designated as MHOM/AR/2016/TcM (DTU: TcV) (MAFFEY et al., 2012).

2.3. Epimastigogenesis

To obtain epimastigotes from the TcM strain, the supernatant of cell culture infected with trypomastigotes was centrifuged at 10,000 *g* for 10 min in Eppendorf™ Centrifuge 5424 R. The supernatant was discarded, 1 mL of fresh medium was added, and the culture was kept at 37 °C in an upright position for one hour. This standard process allows the "swim-up" of clean trypomastigotes, avoiding cellular debris, as previously shown (Romano et al., 2009). Supernatant was separated and placed in 5 mL of Diamond medium (Tryptose 6.25 g. 1 L^{-1}; Tryptone 6.25 g. 1 L^{-1} [Oxoid Limited®]; yeast extract 6.25 g. 1 L^{-1}; potassium dibasic phosphate [K_2HPO_4] 4.02 g. 1 L-1; potassium phosphate monobasic [KH_2PO_4] 4.02 g. 1 L^{-1} [EM®]; sodium Chloride [NaCl] 6.25 g. 1 L^{-1} [Biopack®]) supplemented with penicillin and streptomycin antibiotics and 20% inactivated fetal bovine serum (FBS). After 20 days, the axenic culture was stable in the form of *T. cruzi* epimastigotes.

2.4. Morphometric test

A total of 10 million epimastigotes from both strains (Y and TcM) were fixed with PFA 4% (paraformaldehyde) and examined under an Olympus FV1000 confocal microscope. Digital measurements were performed on individual cells using the morphometry software ImageJ-Fiji (1.51n version National Institute of Health, USA). A total of 100 epimastigotes from both strains were measured in triplicate to study the length of the body cell (Fig. 1C). Data were analyzed with Student's *t*-test for statistical comparison.

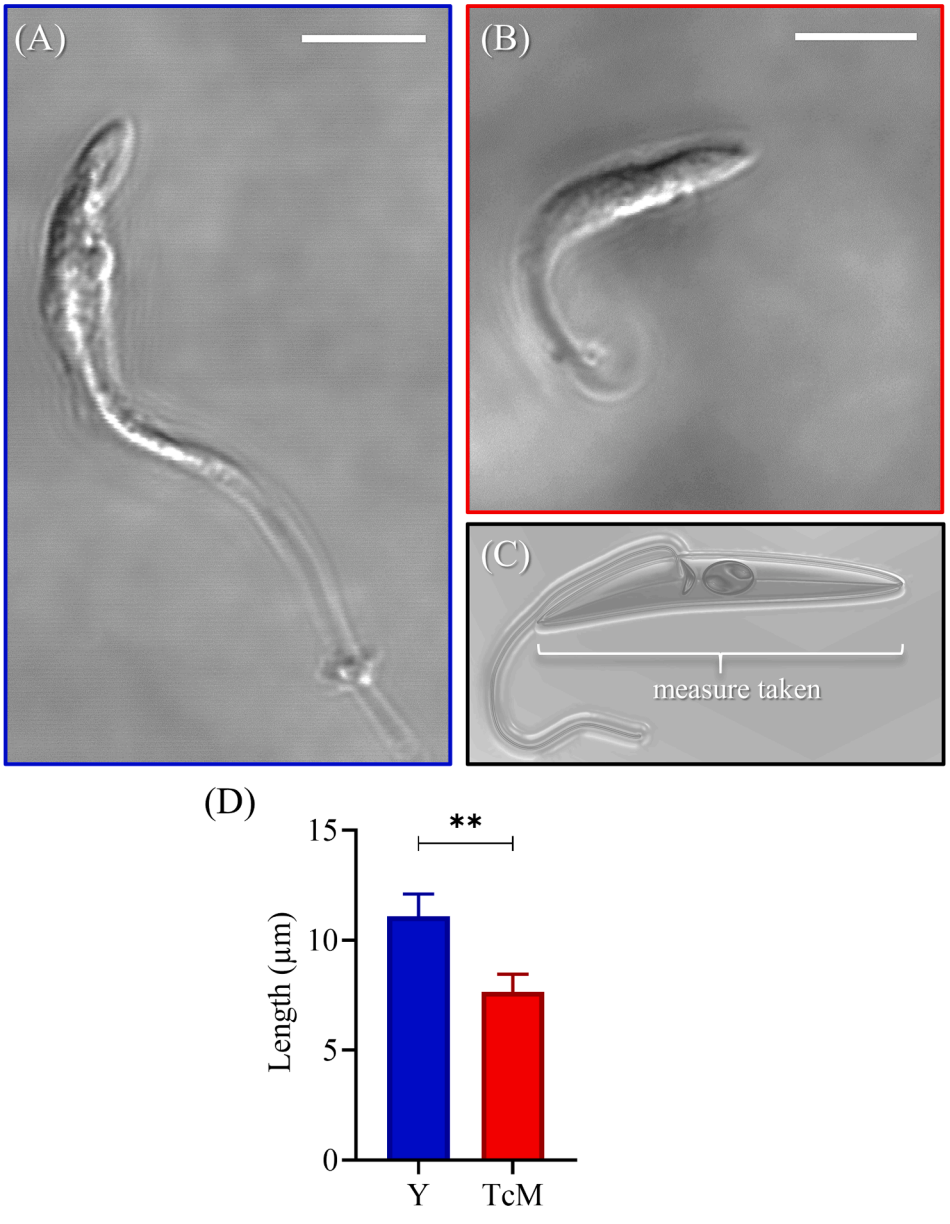

Fig 1. Comparative morphology of *T. cruzi* epimastigotes of the Y and TcM strains. (A and B) Light microscopy images of epimastigote cells from the Y and TcM strains. (C) Segment used for morphometric measurement. (D) Bar graph showing the means ± SD of 100 parasites measured for each condition on three samples from different axenic cultures. A Student's *t*-test was performed with a significance level established by the p-value ≤ 0.001 ***. SD: standard deviation. LA: length average. Scale bar: 10 µm.

2.5. Genetic typing of the TcM isolate

A sample containing 70 million epimastigotes from the Y and TcM strains in the exponential phase previously washed with 1X PBS (Phosphated Buffer Saline solution) was used for the DNA isolation protocol using the DNAzol® reagent (Invitrogen™) as per the manufacturer instructions. The *T. cruzi* Y and TcM strains were genotyped using the PCR-RFLP assay based on the TcSC5D and TcMK polymorphic genes, as previously described by Cosentino & Aguero Cosentino and Agüero, 2012. In brief, the amplification reactions were carried out in a total volume of 25 μl containing 10 pmol of each of the primers (TcSC5D-fwd 5`- GGACGTGGCGTTTGATTTAT-3`, TcSC5D-rev 5`-TCCCATCTTCTTCGTTGACT-3`, Tc-Mev-kinase26-Fw 5`-TTTTTGCATGT-CATTTTGG-3`, Tc-Mev-kinase662-Rv 5`-AGCGGTCTTGTAATGAGCAC-3`), PCR buffer (Invitrogen), 1.6 mM MgCl2, 200 mM dNTPs, 2.5 U Taq polymerase (Invitrogen), and 100 ng of genomic DNA. The cycle conditions were as follows: 94 °C for 4.5 min followed by 35 cycles at 94 °C for 30 s, followed by 30 s at 58 °C and 30 s at 72 °C. Reactions were finished by a cycle of 5 min at 72 °C. To define lineage DTU I, DTU II, DTU III, DTU IV, or DTU V/VI, 20 μl of TcSC5D amplification products (832 bp) were simultaneously digested with 1 U of HpaI (NEB R0105) and 1 U of SphI (NEB R0182) for 1 h at 37 °C. Restriction fragments were then resolved in 2% TBE-agarose gel for 1 h at 5.33 V/cm. To distinguish between TcV and TcVI, 20 μl of TcMK amplification product (457 bp) was digested with 1 U of XhoI (NEB R0146) for 1 h at 37 °C. Restriction fragments were resolved in 2.5% agarose gel for 1.5 h at 5.33 V/cm. Additionally, the TcMK amplification product was sequenced. To do this, 10 μl of the amplification product was incubated for 45 min with 1 U of Exonuclease I (Fermentas, MA, USA) and 10 U of Shrimp Alkaline Phosphatase (Fermentas, MA, USA) at 37 °C. To inactivate the enzymes, samples were incubated for 30 min at 80 °C. Forward and reverse sequencing reactions were performed with Tc-Mev-kinase26-Fw and Tc-Mev-kinase662-Rv primers, respectively.

2.6. Cell lines and culture

H9C2 and HSkM cell lines, derived from muscle tissues, the epithelial Vero C-76 cells, and the fibroblast (MEF) cells were maintained following the manufacturer's conditions of culture as follows: H9c2 (rat embryonic cardiomyocyte cells) (ATCC® CRL1446 ™) were cultured at 37 °C and 5% CO_2 in Dulbecco's Modified Eagle Medium (DMEM) (Gibco®) supplemented with 10% fetal bovine serum, 100 U. mL^{-1} Penicillin + Streptomycin (Gibco®), ciprofloxacin 5 $\mu g.ml^{-1}$ (Roemmers®); HSkM (Human Skeletal Muscle cells), generously donated by Dr. George Truskey (University of. Duke, NC, USA), were cultured at 37 °C and 5% CO_2 in DMEM low glucose (Gibco®) supplemented with 10% FBS, 100 U. mL^{-1} penicillin + streptomycin (Gibco®), ciprofloxacin 5 μg. mL^{-1} (Roemmers®) and SKGM-SINGLE-QUOT-KIT SUPPL & GROWTH FACTORS (sparing insulin) (Lonza®); Vero C-76 cells (ATCC® TL-1456) (African green monkey kidney cells) were cultured at 37 °C and 5% CO_2 with DMEM (Gibco®) supplemented with 3% FBS, 100 U. mL^{-1} penicillin + streptomycin (Gibco®), ciprofloxacin 5 μg. mL^{-1} (Roemmers®); MEF cells (Mouse Embryonic Fibroblasts) were cultured at 37 °C and 5% CO_2 with DMEM supplemented with 3% fetal bovine serum, 100 U. mL^{-1} penicillin + streptomycin (Gibco®), and ciprofloxacin 5 μg. mL^{-1} (Roemmers®).

2.7. Cell infection assays

The four cell lines were plated in 24-well plates on dish coverslips and infected with *T. cruzi* from both DTUs at a multiplicity of infection (MOI) of 10 trypomastigotes per cell for 72 h. Then, cells were fixed with 200 μl in 4% PFA for 30 min at room temperature (RT) and washed three times with 1X PBS (Gibco®). Indirect immunofluorescence (IIF) was performed to label intracellular parasites, as previously described (Romano et al., 2009). Briefly, cells were incubated with 200 μl of 50 mM NH_4Cl for 15 min, and then washed with 1X PBS and incubated with 200 μl PBS-Albumin-Saponin for 20 min at RT to permeate cells. Specific mouse polyclonal serum against *T. cruzi* (1:100) was incubated ON at 4 °C followed by incubation with rabbit anti-mouse Alexa Fluor® 488 (Jackson ImmunoResearch ™) (1:100) for 2 h at 37 °C. After washing, cells were incubated with Rhodamine-Phalloidin (Sigma-Aldrich™) (1:200) for 1 h at 37 °C to mark actin filaments. The coverslips were mounted with Mowiol® (Sigma-Aldrich) with Hoestch® (1:1000) to mark DNA from cores (LifeTechnologies™). Images were quantified using Nikon UpRigth 80i Eclipse fluorescence microscope. The percentage of infected cells was calculated as the number of infected cells with respect to the total number of cells in 20 images taken at 40x for each condition. Data were analyzed with Student's *t*-test for statistical comparison. Three independent experiments were performed in duplicate.

2.8. In vivo infection on immunosuppressed mice

A total of 6 NOD scid gamma mice (NSG mice) per group, generously donated by Dr. Sebastián Real (Instituto de Histología y Embriología de Mendoza, IHEM-CONICET-UNCUYO) were infected under SPF conditions with 10,000 trypomastigotes of each DTU by intraperitoneal (IP) injection. Parasites were taken from a culture of H9c2 cells, purified by swim-up as explained above and suspended in sterile saline solution before inoculation. At different days post-infection (DPI), animals were anesthetized with ketamine (Holliday®)/xylazine (König®) (AF Casassa et al., 2019) dissolved in sterile saline solution, and 5 μl of blood was obtained through puncture of the caudal vein diluted in 0.5 μl of sodium heparin (Duncan®). Blood samples were diluted 1:10 with Lysis buffer (150 mM NH_4Cl; EDTA 0.1 mM; $KHCO_3$ 10 mM) and the number of parasites was counted in a hemocytometer chamber by light microscopy under an Olympus® CX31 microscope as previously shown (AF Casassa et al., 2019). A Mantel-Cox analysis of parasitemia was performed to compare both groups. At the endpoint, animals were euthanized by strong sedation with a ketamine/xylazine injection followed by cervical dislocation. The endpoint was performed when animals showed any signal of pain and suffering. Heart and liver of each mouse were dissected and fixed for histological studies. All animal procedures were carried out in accordance with the Guiding Principles in the Care and Use of Animals of the US National Institute of Health. All procedures were approved by the Institutional Animal Care and Use Committee of the School of Medical Science, Universidad Nacional de Cuyo (Protocol approval N° 107/2017).

2.9. Histologic analysis

The livers and hearts of mice, representative of epithelial and muscle cells, respectively, from each group were dissected and immediately washed three times with 1X PBS for 5 min, fixed with 4% PFA for 24 h, and then washed three times with 1X PBS and kept in 70% alcohol to begin dehydration of the organ. All tissues were subjected to increasing dilutions of alcohol starting with three washes of 10 min at 70%, 90%, 96%, and 100%, one hour of xylene, followed by half an hour of intermediate solution ((Melo and Brener, 1978-50) of xylene/paraffin in a stove at 60 °C. After three washes of 30 min with paraffin, samples were cooled at RT and assembled to make cuts in microtome (MICROM HM325). Then 6 cuts of 5 μm thickness were made at 70 μm of spacing to minimize overlaps of amastigote nests. The sections were mounted on slides and stained using the hematoxylin (Vector®)/eosin protocol (Biopur®). A total of 25 fields were counted in 40x magnitude per cut under a Nikon Upright 80i eclipse optical microscope (Abegg et al., 2017). Number of amastigote nests in 150 fields in liver and heart from each strain was obtained and compared using Student's *t*-test for statistical analysis.

2.10. Analysis of the benznidazole effect on epimastigote forms

Ten million epimastigotes per condition were treated with 100 μM of

BNZ or DMSO (control) in complete Diamond medium for 3 days and then centrifuged at 10,000 *g* for 3 min, washed with PBS 1X three times, and cultured in fresh medium without the drug for an additional time of up to 10 days. Live motility of the epimastigotes was quantified at 3, 7, and 10 days post-treatment in a Neubauer hemocytometric chamber under the light of an optical microscope. Data were analyzed with the unpaired two-way Student's *t*-test.

2.11. Determination of IC_{50} for benznidazole on epimastigote forms

Cultures of epimastigotes at the exponential phase were obtained from complete Diamond medium supplemented with 10% FBS for the Y strain (TcII) and 20% for the TcM strain (TcV) due to its slow growth. Epimastigotes were exposed to increasing concentrations of BNZ from 0.1 to 250 μM for 72 h. BNZ (ELEA laboratory) stock was prepared in dimethylsulfoxide (DMSO) at 1, 25, and 1000 mM and stored at –20 °C. All conditions were brought to the same percentage of DMSO. Live motility of the epimastigotes was quantified in Neubauer hemocytometric chamber under optical microscopy with the Olympus CX31 at the end of the experiment. IC_{50} values were estimated by the analysis of means adjusting to a dose-response curve. Data were analyzed with the unpaired two-way Student's *t*-test. Three independent trials were performed in triplicate.

2.12. Transmission electron microscopy

Epimastigotes treated with the estimated IC_{50} concentrations for 72 h were centrifuged at 10,000 *g* for 3 min and washed three times with 1X PBS. The samples were fixed in 2.5% glutaraldehyde (Pelco International, CA, USA) in 0.1 M sodium cacodylate buffer for 2 h at 10 °C, immersed in 1% agarose (Sigma-Aldrich®), and immediately centrifuged at high speed to obtain the solid pellet. Each set was washed in the same buffer, post-fixed in 1% OsO_4 for 1 h at RT, dehydrated in a graded acetone series, and embedded in low-viscosity epoxy resin (Pelco International), as described previously (Virreira et al., 2006). Polymerization was performed for 48 h at 70 °C. Ultrathin sections with interference color gray were cut by an ultramicrotome (Ultracut R; Leica, Wien, Austria), mounted on grids, and stained with uranyl acetate and lead citrate (Macchiaverna et al., 2018). Grids were examined by TEM under a Zeiss 900 electronic microscope (Jena, Germany).

2.13. Determination of IC_{50} for benznidazole on amastigote forms

H9c2 cells were plated in 24-well plates on dish coverslips and infected with trypomastigotes of each strain at a MOI of 10. After 24 h, samples were washed three times with 1X PBS solution to remove the trypomastigotes that had not entered the cells. Fresh medium was added at increasing concentrations of BNZ, from 0.1 to 100 μM, or DMSO (control) and incubated for 48 h before fixing. Intracellular amastigotes were labeled by IIF following the procedure explained above. Fluorescent images were obtained under a Nikon UpRight 80i Eclipse fluorescence microscope for each condition. Number of amastigotes per infected cell was quantified from 20 images and displayed as the percentage of growth in comparison with the controls. IC_{50} was calculated using the mean number of amastigotes per infected cell at the increased concentrations of BNZ. Data were obtained from three independent trials in duplicate and analyzed by Student's *t*-test.

2.14. Statistical and imaging software

All statistical analyses were performed with GraphPad Prism version 8.0.0 for Windows (GraphPad Software, San Diego, California USA, www.graphpad.com). Figures were made with Microsoft Office PowerPoint 2019 for windows version 64-bits, and image processing with Image J version 1.53 m (Fiji).

3. Results

3.1. Isolation of a new T. cruzi strain and molecular characterization

The new *T. cruzi* strain was isolated from a blood sample obtained from a patient with chronic CD that suffered an acute reactivation of the infection due to immunosuppressive therapy. The sample was taken after positive parasitemia was confirmed by standard procedures in the clinical laboratory and before the initiation of the trypanocidal therapy with BNZ (see ethical statement and *T. cruzi* isolation in Materials and Methods for details). Blood samples were incubated with Vero cells first, but very low infection was observed on these cells. Next, H9c2 cells, also used for *T. cruzi* culture, were employed and better results were achieved. After washing out free parasites and culturing cells for several days, we noted that amastigotes were visible in the host cell cytoplasm and free trypomastigotes in the medium. Interestingly, in agreement with previously published data that demonstrated the inhibition of host cell apoptosis by *T. cruzi* infection (Cortez et al., 2012), few dead host cells were observed in the culture even at higher culture confluence.

An aliquot of trypomastigotes obtained in the culture was frozen to prevent changes associated with the passages in cell culture. Another aliquot was used to maintain the culture in H9c2 cells, and a third one was used to obtain epimastigotes by placing trypomastigotes in Diamond medium. Although initially a low number of trypomastigotes was transformed into epimastigotes, the number of TcM epimastigotes increased significantly when the medium was supplemented with 20% FBS. Epimastigotes and trypomastigotes from TcM strain were then used to perform different experiments to study their properties in comparison with the *T. cruzi* Y strain, whose biological behavior both *in vitro* and *in vivo* has been well characterized (AF Casassa et al., 2019; SJ Martinez et al., 2020; Recommendations from a satellite meeting 1999).

3.2. TcM epimastigotes differ in size from those of the Y strain

As a first approach, epimastigotes from both strains were subjected to morphometric analysis by optical microscopy. Parasites of the TcM strain displayed a reduced size in comparison with those from the Y strain (Fig. 1A and B). The length of TcM cell body (without the free extreme of the flagellum, Fig. 1C) was significantly shorter than that of TcY with an average length of 7.65 ± 0.8 μm against 11.1 ± 1.01 μm, respectively (Fig. 1D).

3.3. TcM belongs to DTU TcV as revealed by genotyping

The genetic background of the TcM strain was then assessed to classify this new isolate into a specific DTU. Parasites were genotyped by PCR-RFLP using the polymorphic markers *TcSC5D* and *TcMK,* as previously described by Cosentino & Aguero (Cosentino and Agüero, 2012). After *TcSC5D* amplification, all strains tested gave a unique 832-bp band (not shown). Double digestion of this band with restriction enzymes *SphI* and *HpaI* showed that the TcM strain belonged either to the TcV or TcVI lineage (Fig. 2A, lane 7). As expected, Y parasites displayed the characteristic digestion pattern of the TcII lineage (Fig. 2A, lane 6). A second PCR-RFLP assay using the *TcMK* product digested with *XhoI* showed that TcM belongs to the TcV lineage (Fig. 2B, lane 4). Furthermore, direct sequencing of the PCR products revealed the expected homozygous and heterozygous peaks for DTU TcV at the key informative SNPs used for typing (see Supplementary Figure 1, strain typing sequencing). In particular, the 'C/T' heterozygosity of the SNP at position 618 is the telltale of strains from DTU TcV (all tested strains from DTU TcVI are homozygous for 'C' at this position)(17). The genotypic identity of the TcM strain in the TcV lineage was not surprising because of the known predominance of this lineage in clinical and domestic isolates from Argentina (LP Quebrada Palacio et al., 2018; Macchiaverna et al., 2018).

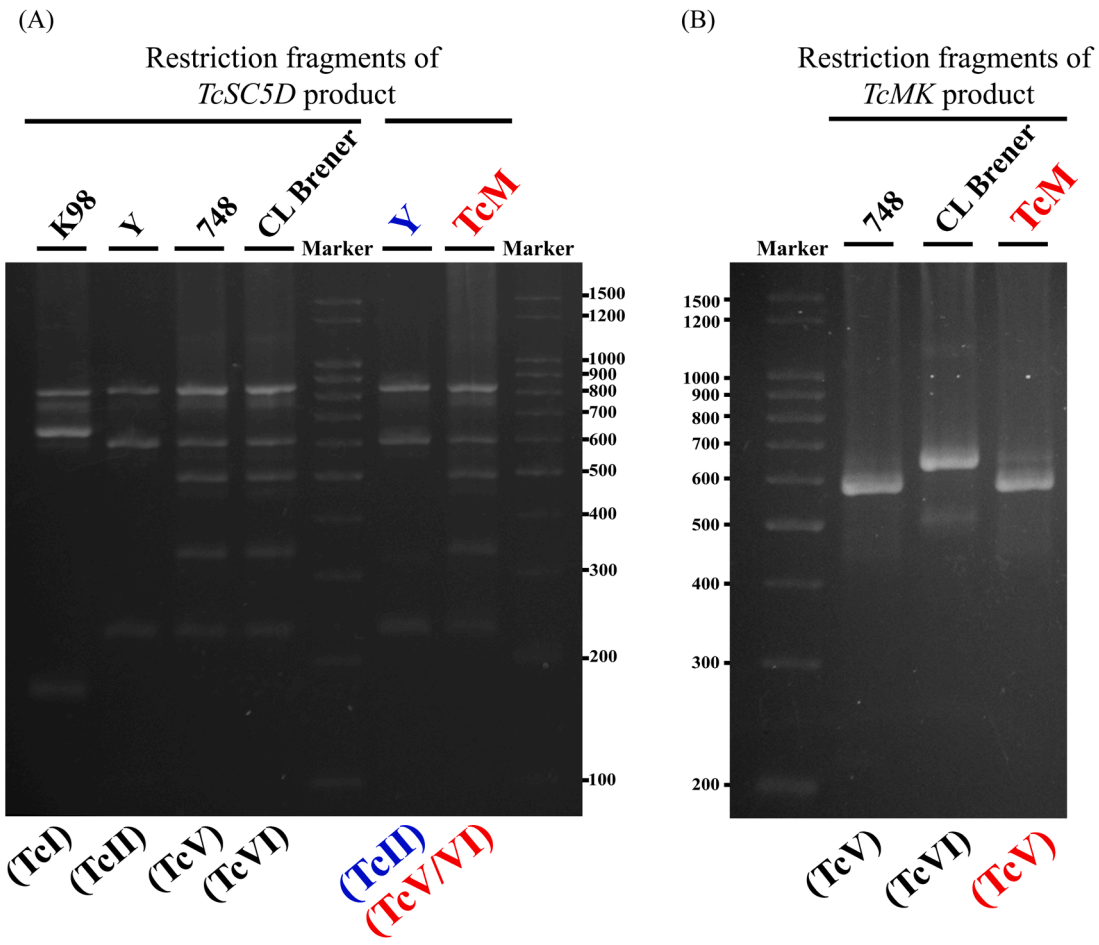

Fig 2. PCR-RFLP typing of TcM strain parasites. (A) Restriction fragment length of the TcSC5D amplification product. The 832-bp product was digested with SphI/HapI and the resulting fragments were resolved in 2% TBE-agarose gel. Lines 1–4 correspond to DNA from TcI, TcII, TcV, and TcVI lineages, respectively. Line 5: molecular size marker. Line 6 and 7 correspond to DNA from Y and TcM strains, respectively. Line 8: molecular size marker. (B) Restriction fragment length of the TcMK product. The 637-bp product was digested with XhoI and analyzed in 2.5 TBE-agarose gel. Line 1: molecular size marker. Lines 2 and 3 correspond to DNA from TcV and TcVI lineages. Line 4 corresponds to DNA from TcM strain. The analysis was performed in three samples of different cell cultures.

3.4. TcM displays more infectivity in muscle cells than in others

In vitro and *in vivo* assays were performed to characterize the infection capacity displayed by the TcM strain in comparison with the *T. cruzi* Y strain. Different cell lines derived from epithelial, connective, and muscle tissues were used as host cells for the *in vitro* infections. After 72 h of infection, infected cells were fixed, and parasites were detected by indirect immunofluorescence using a primary anti-*T. cruzi* antibody followed by detection with a secondary antibody bound to a green fluorophore. To facilitate visualization, host cell microfilaments were stained with phalloidin rhodamine, as previously described (Romano et al., 2009) (see details in Materials and Methods). As shown in Fig. 3A both TcM and Y strains displayed a uniformly high degree of infection in both H9c2 and HSkM cells derived from rat heart myoblasts and human skeletal muscle, respectively. In contrast, the TcM strain displayed very low infection rates in the non-muscular Vero or MEF cells lines.

Quantification studies showed that the percentage of infected cells was almost 10 and 7.5 times lower in Vero and MEF cells exposed to TcM in comparison with the Y strain, respectively (87.8 ± 2.95% against 8.9 ± 1.88% for Vero cells and 44.45 ± 11.77% against 5.97 ± 3.83% for MEF cells), while in muscle-derived cells both strains displayed similar infectivity. Furthermore, the level of infection displayed by the Y strain was similar for all host cell lines tested, with an average of more than 40% of infected cells (Fig. 3B). These data showed the major affinity of TcM for muscle-derived tissues in contrast to TcY, which behaves as a reticulotropic strain, as previously shown (AF Casassa et al., 2019).

3.5. The TcM strain displays reduced virulence and chronic behavior in NSG mice

Infectivity was also studied in animal models by using NSG (NOD scid gamma mouse) mice. Trypomastigotes from the TcM and Y strains were inoculated in animals by IP injection, and the course of the infection was analyzed by parasitemia and survival. A fast increase in parasitemia values was observed in mice infected with the Y strain, reaching the peak around 10 days post-infection (DPI) (Fig. 4A). In contrast, animals infected with the TcM strain developed a slow infection with the beginning of measurable parasitemia at 20 DPI and reaching the peak at 60 DPI. Because NSG mice are immunodeficient (lacking mature T cells, B cells, and natural killer [NK] cells), infections with either strain ultimately led to death in all animals at the parasitemia peak (13 DPI for Y strain and between 40 and 58 DPI for the TcM strain, see Fig. 4B). The level of tissue parasitism was further analyzed in the hearts and livers of mice by standard histological procedures. Significant differences were found in the number of amastigote nests found in tissues (Fig. 4C and D). Remarkably, a higher number of nests in the cardiac tissue were observed in TcM-infected mice than in mice infected with Y. In contrast, in hepatic tissue, very low infection rates were observed in animals infected with the TcM strain. The data also showed that a significant higher number of amastigote nests were developed in the liver of Y-infected mice than in the heart of the same animals, in concordance with previous reports (AF Casassa et al., 2019). Taken together, both *in vitro* and *in vivo* studies highlighted the preference of

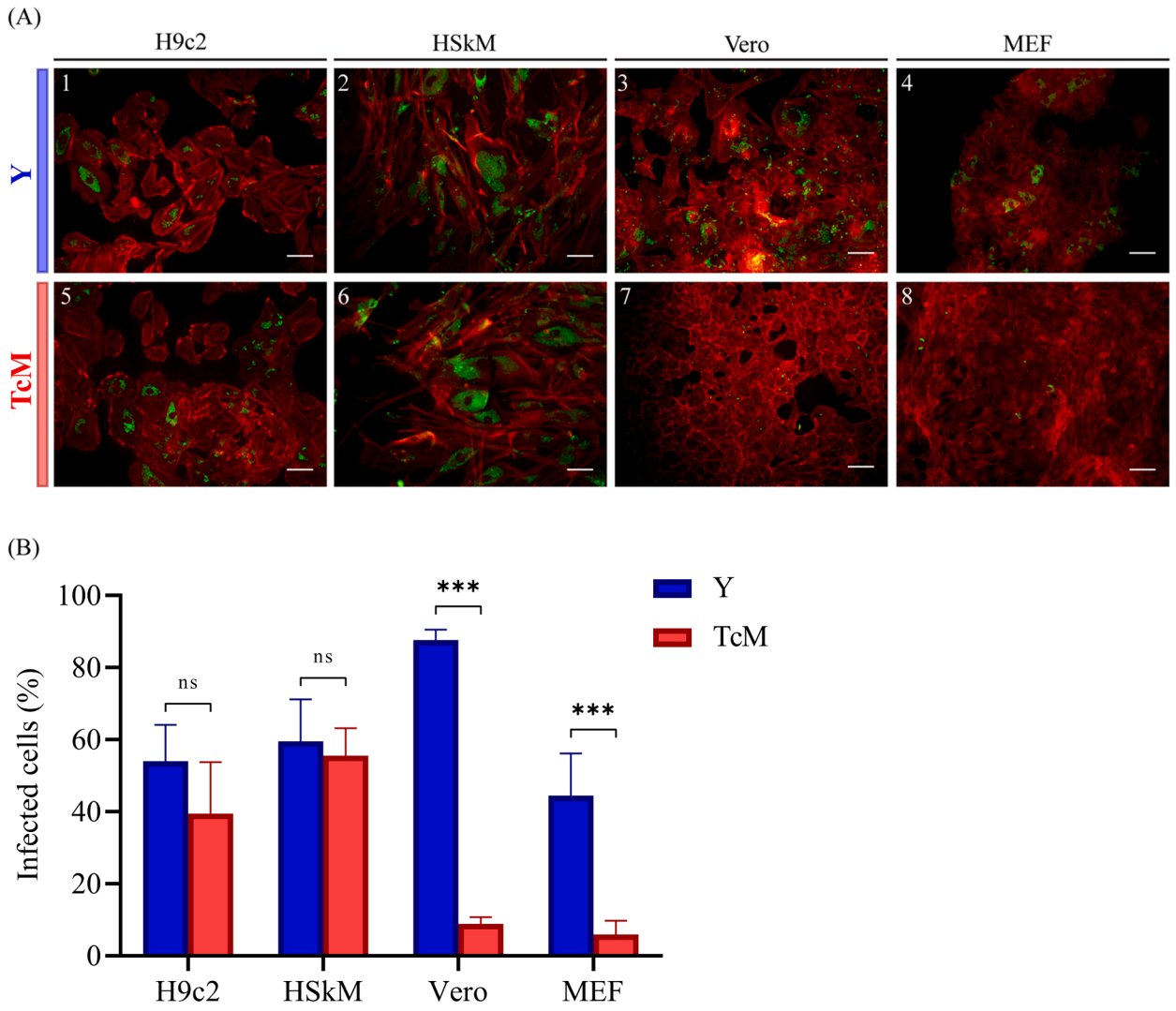

Fig 3. Infectivity of TcM and Y strains in different cell types. H9c2 and HSkM (muscular cells); Vero (epithelial cells) and MEF cells (fibroblasts) were infected for 48 h (MOI= 20) with trypomastigotes of *T. cruzi* from each strain following by fixation and preparation for fluorescence microscopy analysis. Actin filaments of host cells were labeled with the rhodamine phalloidin marker (red) and parasites detected by IIF by using a specific antibody against *T. cruzi* followed by a secondary antibody labeled in green. (A) Confocal images of samples from Y (Pérez-Molina and Molina, 2018; Tyler and Engman, 2001; Osorio et al., 2012, 4) and TcM (5; Nunes et al., 2013; Andrade et al., 1999; Vago et al., 2000) infected cells. (B) Percentage of infected cells quantified from each sample. Bars represent means ± SD of two independent experiments performed in duplicate. The means were analyzed with Student's *t*-test for statistical comparison with a significance level established by the p-value ≤ 0.001 ***. Scale bar: 40 μm.

TcM strain for muscle cells and tissues and the reduced affinity for other cell types in contrast to the Y strain. These data are in agreement with the clinical signs of the patient, who also displayed a higher level of infection in skeletal muscle (data not shown).

3.6. The TcM strain is susceptible to benznidazole

BNZ is one of the two drugs approved for the treatment of CD. Previous data showed high variability of *T. cruzi* strains and isolates in the susceptibility to this drug (LP Quebrada Palacio et al., 2018). To study the level of susceptibility of TcM to BNZ, the growth of epimastigotes, generated from trypomastigotes *in vitro* (see details in Materials and Methods), was analyzed in the presence of BNZ and compared with the Y strain. Epimastigotes of both strains were incubated in control medium or in the presence of 100 μM of BNZ for 3 days followed by a chase with control medium for an additional time of 10 days (see the scheme in Fig. 5A and details in Materials and Methods).

The growth curves displayed by both strains were very similar in control conditions (for TcM, the medium was supplemented with 20% FBS, as otherwise parasites do not grow properly, see Fig. 5B, upper curves). As expected, growth stopped or was significantly reduced during exposure to BNZ, indicating that in these conditions the drug affected the replication of the strains in a similar way. However, when normal growth conditions were restituted, epimastigotes of the Y strain resumed growth whereas the growth curve for TcM parasites remained flattened and displayed a significantly smaller number of parasites in the culture on day 10 (Fig. 5B, lower curves). The low recovery capacity after BNZ treatment of the TcM strain indicated that this strain is more sensitive to the BNZ treatment than the Y strain, which was previously classified as a partially resistant strain (AF Casassa et al., 2019; Spurr, 1969; REYNOLDS, 1963). To confirm these data, the IC_{50} of BNZ for each strain was calculated by quantification of growth at increased concentrations of BNZ for 72 h. The data showed that the IC_{50} for the Y strain was 32.75 ± 1.76 μM, similar to previously reported values (Chuenkova and PereiraPerrin, 2009), while the IC_{50} for the TcM strain was 9.52 ± 1.09 μM (Fig. 6A and B).

Although the exact mechanism of action of BNZ has not been totally elucidated yet, it has been shown that DNA damage in *T. cruzi* is part of

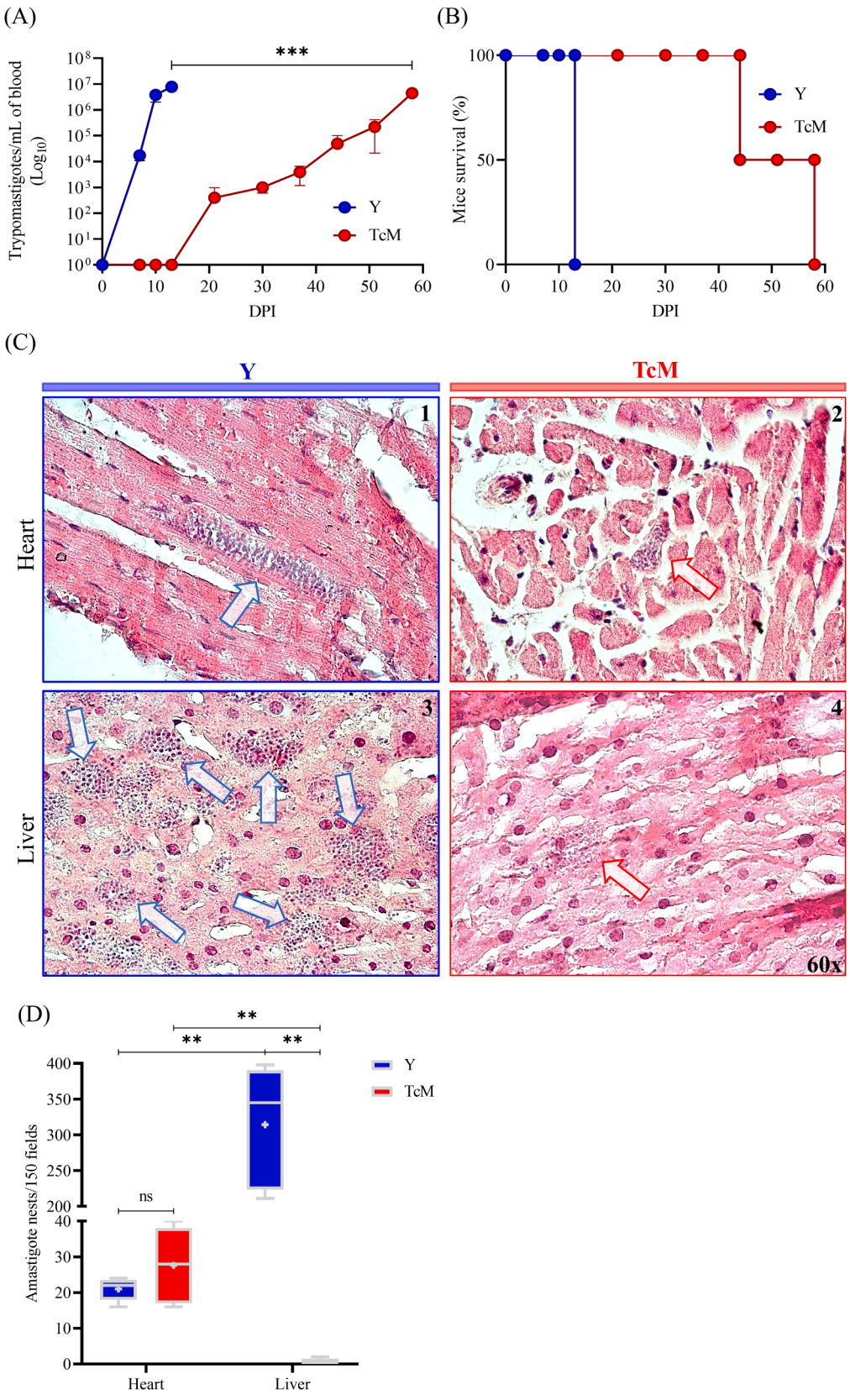

Fig 4. Acute infections in immunosuppressed NSG mice. Two groups of 6 mice were infected with 10^3 trypomastigotes from each strain. Parasitemias were quantified every 3 days during the first 2 weeks and once a week up to 58 days post-infection. The hearts and livers of euthanized animals were dissected for histological studies. All procedures are described in Materials and Methods. (A) Curves of parasitemia displayed by TcY and TcM strains. Data represent the means ± SD of the individuals infected with each strain. (B) Survival rate of individuals. A Mantel-Cox analysis was performed to compare data, p-value ≤ 0.001***. (C) Images depict histological sections of the heart and liver infected with each *T. cruzi* strain and stained with H&E. Black arrows indicate amastigote nests, (D) Number of amastigote nests quantified from the histological samples. The graph shows the median obtained from Y or TcM strains in each tissue. A Mann-Whitney analysis was performed to compare all medians by condition, significance level established by the p-value ≤ 0.05* and $p \leq 0.01$**, ns: not significant. Scale bar: 30 μm.

the cytotoxic effect of this compound (Rajão et al., 2014). Therefore, the effect of BNZ on the ultrastructure of treated parasites was studied. Epimastigotes from TcM and TcY strains were treated with BNZ at their respective IC_{50} values for 72 h and then fixed and processed by TEM. Analysis of micrographs showed an increased number of large vesicles that resembled autophagosomes (AP) in the cytoplasm of treated parasites from both strains, while vacuole (V) and lipid droplets (LD) showed no significant changes (Fig. 6C). Interestingly, the nucleus (N) and

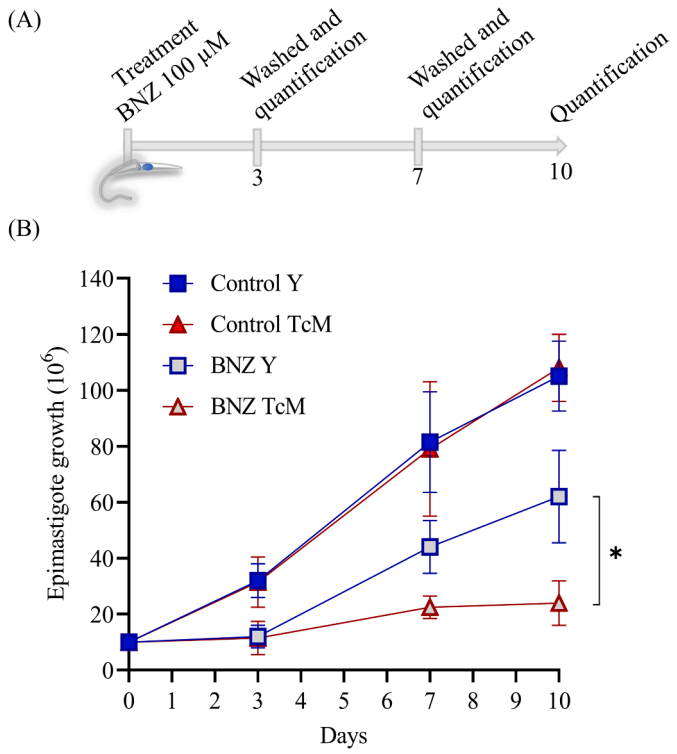

Fig 5. Susceptibility to BNZ treatment in epimastigote forms. A total of 10×10^6 epimastigotes from each strain were treated with 100 µM BNZ or 1% DMSO (controls) for 72 h and growth was analyzed by quantification in a Neubauer chamber. (A) Timeline scheme of the experiment. (B) Growth curves of epimastigotes from each strain in the different conditions.. Data represent the means ± SD from three independent trials by triplicate. The conditions were analyzed with the unpaired two-way Student's *t*-test. Significance level established by the p-value ≤ 0.05*.

kinetoplasts (K) from both strains displayed some deformation compared to controls, showing that BNZ produces a slight effect on the ultrastructure of nuclear or mitochondrial DNA at these conditions. Moreover, no difference was observed between strains at the ultrastructural level upon treatment with BNZ, supporting the idea that differential sensitivity to BNZ is not associated with major ultrastructural changes in these strains. Besides, the presence of autophagosomes reveals the cellular stress suffered by the treated parasites, which increased autophagy as a survival response, as previously reported (Menna-Barreto, 2019).

In another set of experiments, the effect of BNZ was studied in amastigote replication by quantifying the IC_{50} of BNZ for each strain on H9c2 heart myoblasts. Trypomastigotes from TcM and Y strains were used to infect H9c2 cells for 24 h. After washing to remove free parasites in the medium, cells were treated at increasing concentrations of BNZ for 72 h before fixation (see details in Materials and Methods). Intracellular parasites were detected by IIF assay and the rhodamine-phalloidine marker was used to stain host cell actin microfilaments and then analyzed by fluorescence microscopy. As expected, the intracellular parasites decreased when cells were subjected to BNZ from 0.1 to 100 µM (Fig. 7A). The number of parasites per cell in each condition is presented in Fig. 7B and C. The IC_{50} values calculated were 21.17 ± 1.14 µM and 15.91 ± 1.9 µM for the Y and TcM strains, respectively. Similar to the studies on epimastigotes, the effectiveness of BNZ in amastigote forms was significantly higher in the TcM strain than in the Y strain. Altogether, these data confirm the major susceptibility of TcM to BNZ.

4. Discussion

One of the main weaknesses in the pre-clinical analysis of new drugs for CD is that they are performed on *T. cruzi* strains initially isolated from the natural cycle but then maintained for years in laboratory conditions, far away from the real natural parasite-host cycle. The aim of this work was to isolate a *T. cruzi* strain from a clinical sample and characterize its biological properties in comparison with a laboratory strain. The new isolate was designated TcM, because of its origin in Mendoza city (Argentina). TcM was then characterized at different levels in comparison with the Y strain, a widely available *T. cruzi* strain used as a reference strain in many research laboratories around the world. One of the first differences observed between Y and TcM parasites was the size of the epimastigote body. TcM cells displayed a significantly smaller size than those of the Y strain, a difference that was easy to see by optical microscopy (Fig. 1). Besides genotyping, morphometric measurements can be used as simple tools leading to the first characterization of *T. cruzi* strains (De Diego et al., 1991). The cell body size can influence parasite motility, which is important to the efficiency of invasion to host cells. In a recently published work, Arias-del-Angel and colleagues showed that *T. cruzi* is capable of modifying its motility patterns to increase its invasion efficiency (Arias-del-Angel et al., 2020). The lower cell body of TcM could influence the motility of trypomastigotes in the presence of host cells, resulting in lower infectivity in comparison with the Y strain, which possesses a higher cell body.

Another feature studied in this work was cellular tropism. Initial experiments showed that the TcM strain displayed very low infection and replication rates in Vero cells in comparison with the Y strain. Vero cells are used in many laboratories as the standard protocol to maintain the *T. cruzi* culture. Further infection studies using host cells derived from different tissues demonstrated that TcM displayed low infectivity in Vero and MEF cells but higher infection rates in the muscle-derived H9c2 cell line (neonatal rat myoblasts) and in HSkM cells (human skeletal myoblasts). These results correlated with the higher number of amastigote nests of TcM in the mouse cardiac tissue *in vivo*. The myotrophic behavior of TcM can be correlated to the type of pathology produced. It has been demonstrated that the persistence of *T. cruzi* in specific organs activates a chronic inflammatory process responsible for tissue damage (Fernandes and Andrews, 2012). In agreement with this, an intense inflammatory process was found in the gastrocnemius muscle (calf) in the patient during the reactivation of the infection (data not shown), thus confirming the affinity of this strain for muscle tissues in human infection too. In contrast, the Y strain displayed high infectivity of different cell classes, namely epithelial, muscular, and connective derived cells. The higher infection rate displayed by the Y strain in Vero cells could be due to the long-term maintenance of this strain as a lab culture and the fact that it has been replicated in Vero cells for a long time, resulting in the adaptation of the strain to living and replicating in this epithelial cell. The Y strain was isolated from an acute human case from Marília (São Paulo, Brazil) in 1950. A striking feature of the Y strain was the high number of amastigote nests found in the liver of mice. In agreement with these data, extremely high parasitism of the Y strain in the liver, spleen, and bone marrow was shown in a previous study (Melo and Brener, 1978). Other authors also confirmed the reticular tropism of this strain (Vanrell et al., 2017; Filardi and Brener, 1984; Bahia et al., 2012).

Infectivity assessments by an *in vivo* test in immunosuppressed mice (Fig. 4) showed that, in agreement with our previous results (AF Casassa et al., 2019), the Y strain developed an acute infection with high parasitemia in the first week post-infection and mortality as early as 13 DPI. In contrast, infection with the TcM strain displayed delayed parasitemia and mortality. Hence, it can be predicted that this new strain would behave as a chronic strain in other infection models (such as non-immunodeficient mice). Notably, although the environment and hosts were the same for both strains, this study shows the capacity of each strain to produce a different infection even in an

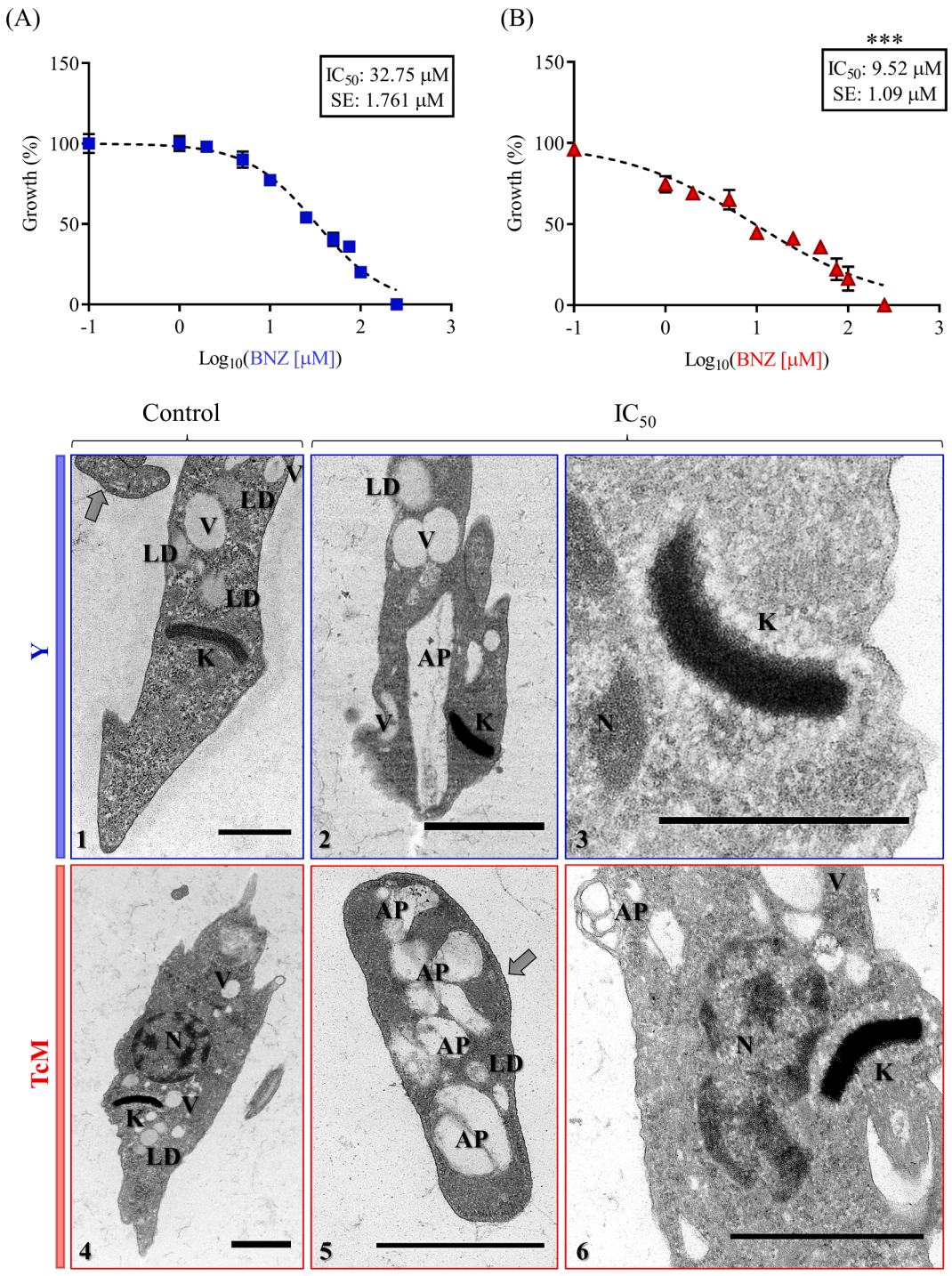

Fig 6. Determination of IC_{50} and assessment of cellular structure changes in BNZ treatment. (A and B) Growth curves of epimastigotes from each strain displayed in the presence of increasing concentrations of BNZ (0.1–250 µM) for 72 h at 28 °C. The untreated control (2% DMSO) was considered as 100% growth and the treatment values were relativized to the control. Graphics show the means ± SE of three independent tests represented on a logarithmic scale with trend line adjustment. The IC50 obtained from each strain was analyzed with a two-way unpaired Student's *t*-test. The significance level was established by the p-value ≤ 0.001***. SE: standard error. (C) TEM images showing the cellular ultrastructure of the epimastigotes under control conditions ((Pérez-Molina and Molina, 2018) and (4)) or at the estimated IC_{50} concentration ((Tyler and Engman, 2001; Osorio et al., 2012, 5), and (Nunes et al., 2013)) for each strain. Both treated strains presented the same cytoplasmic disorganization, showing an increase in autophagosomes (AP) and deformation in the kinetoplast (K) and nucleus (N). Vacuole (V) and lipid droplets (LD) showed no significant changes; black arrow shows cytoskeleton microtubules.

immunosuppressed model such as NSG mice. In other words, the Y strain was more virulent than the TcM strain, demonstrated by the fact that this strain killed 100% of mice in a very short time (13 days) (Fig. 4). It is noteworthy that this aggressive infection and fast progression to death were similar to those caused by the same strain in another model of immunosuppressed mice (AF Casassa et al., 2019). Note that the Y strain requires a high degree of multiplication to produce the fast increase in the parasitemia levels. In this sense, the large pool of nutrients present in the liver favored the supply of food to maintain parasite division at this level.

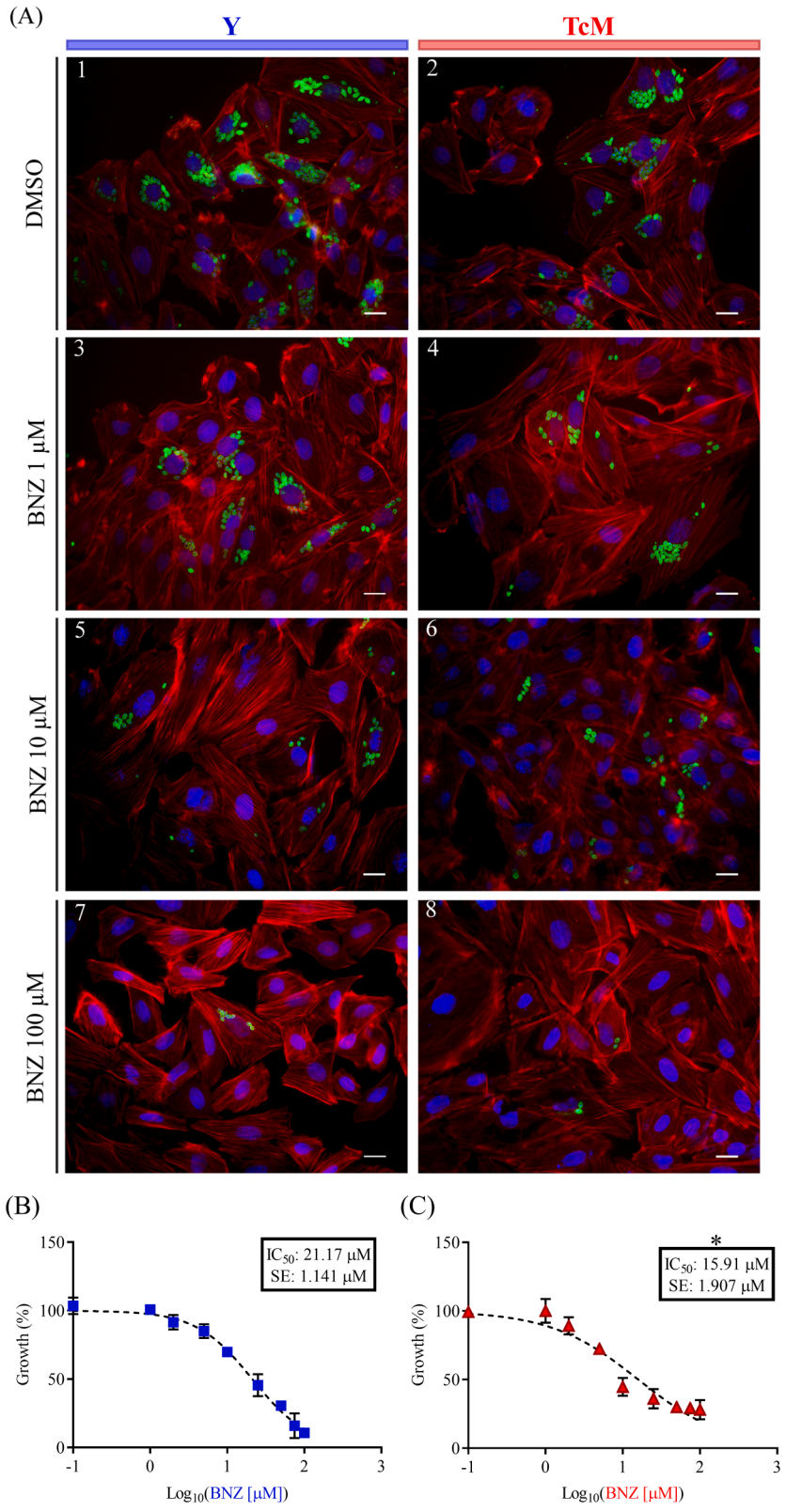

Fig 7. Susceptibility of BNZ treatment in amastigote forms. Infections in H9c2 cells with each strain were performed for 24 h with a MOI of 10 followed by treatment at increasing concentrations [0.1, 1, 2, 5, 10, 25, 50, 75, 100 µM] of BNZ for 48 h. (A) Confocal images depicts the level of infection observed at the indicated conditions from Y and TcM strains. Actin filaments of host cells were labeled with the rhodamine phalloidin marker (red) and amastigotes detected by IIF by using a specific antibody against *T. cruzi* followed by a secondary antibody labeled in green. Nuclei of host cells and amastigotes were stained with Hoechst (blue). (B and C) Percentage of growth and estimation of IC_{50} from Y and TcM strains in a logarithmic scale. Data show the means ± SE of three independent trials in duplicate. The IC_{50} values were analyzed by a Student's *t*-test with a significance level established by p-value ≤ 0.05*. SE: standard error. Scale bar: 20 μm.

The study of susceptibility of TcM to BNZ completes the characterization of this strain, mainly given the existence of *T. cruzi* strains resistant to BNZ treatment (Nunes et al., 2013; Meymandi et al., 2017; Velásquez et al., 2014; Rajão et al., 2014, Campos et al., 2014). The analysis of BNZ susceptibility in both strains showed that epimastigotes of the TcM strain were three times more susceptible to BNZ than those of the Y strain (Fig. 5). Moreover, the epimastigotes of the Y strain easily recovered replication upon washout of the drug, indicating that the mechanisms of cellular detoxification of this strain were more efficient than those of the TcM strain. Given that some enzymatic systems to resist oxidative stress are located in mitochondria, we further investigated the cellular ultrastructure of each strain treated at the IC50 by TEM (Fig. 6).

Detailed analysis of the microscopy images did not reveal any morphological changes suffered by the cells upon treatment with BNZ, mainly at kinetoplasts, the mitochondrial compartment of trypanosomatids. Notably, major changes were observed in the cytoplasm with an increased number of vacuoles and autophagy-like structures (Vanrell et al., 2017), which could have indicated either an autophagy survival process or an autophagy cell death mechanism. A previous study also found myelin-like structures, autophagolyosomes and other cellular abnormalities in BNZ-treated parasites (LP Quebrada Palacio et al., 2018). Other trypanocidal compounds (naphthoquinones and naphthoimidazoles) displayed a similar autophagy-death phenotype (Penin et al., 1996; Brenière et al., 2016). Nevertheless, more studies will be necessary to confirm these observations.

Genetic typing markers positioned the TcM strain within the *T. cruzi* evolutionary lineage V (DTU: TcV) (Fig. 2). According to the study by Breniere and coworkers (de Figueiredo Diniz et al., 2018), except for DTU TcI prevailing in many countries of America (North, Central, and South), DTU TcII is the second most frequent DTU in human infection in Brazil and the hybrid lineages TcV and TcVI are the most frequent in human infection in Argentina and other countries of South America, such as Bolivia, Paraguay, and Chile. Furthermore, the predominance of TcV in new *T. cruzi* isolates was reported in studies performed in Argentina (LP Quebrada Palacio et al., 2018; Macchiaverna et al., 2018). In a previous study, it was demonstrated that TcV isolates exhibit divergent responses to benznidazole and that this difference was related to the differential expression of anti-oxidant proteins: mitochondrial superoxide dismutase and tryparedoxin peroxidase (LP Quebrada Palacio et al., 2018). These authors divided the TcV isolates into two subgroups according to their susceptibility to BNZ and found differences in the infection they developed in mice, with the susceptible strain developing higher parasitemia and mortality rates than the resistant strain. They also showed that BNZ susceptibility/resistance in epimastigotes correlated with the pattern obtained in intracellular amastigotes and trypomastigotes (Quebrada Palacio et al., 2018). Similarly, here we showed that TcM (TcV) is more susceptible to BNZ than Y (TcII) in both epimastigotes and amastigotes. However, TcM amastigotes behaved as a BNZ-resistant strain according to the hit criteria for Chagas disease (IC50<10 μM) defined by Katsuno and co-workers (Katsuno et al., 2015). Remarkably, TcM displayed lower parasitemia and mortality in the acute period in mice, similarly to the BNZ-resistant BOL FC10A strain reported in the Quebrada-Palacio study. Despite the possible technical differences between both studies, a comparison between the TcV strains resulted in important intra-lineage differences concerning BNZ susceptibility and virulence in mice infection. However, a weak connection may be observed in the sense that TcV strains more resistant to BNZ develop a less aggressive infection in mice in contrast to BNZ-susceptible parasites. However, this idea would not be the rule in the case of the Y strain from DTU TcII, which displayed more resistance to BNZ and developed a very aggressive infection in mice. More studies are needed to confirm these relationships. Moreover, host immune responses that depend on the genetic background of the host add a new level of complexity that has to be considered, as discussed in our recent revision (SJ Martinez et al., 2020).

To conclude, data have so far shown that the correlation of specific DTUs with parameters like chronic morbidity, risk of reactivation, or clinical presentation of Chagas is controversial. However, we observed that there is a relationship between the type of infection developed in the patient and the behavior of the isolate in the laboratory. This observation leads us to propose, based on the data available to date, that one of the best ways to predict the clinical outcome of Chagas in a patient would be the isolation of the parasites that cause the infection and the study of its properties through standardized tests. Such tests would give information about tissue tropism, virulence, drug susceptibility, and tendency to chronicity, among others. Other parameters, such as the possibility of mixed infections and host immune responses, will need also to be considered in the future. This precision medicine, although difficult, will make it possible to make better decisions in the management of the patient with Chagas disease.

Declaration of Competing Interest

The authors declare that they have no known competing financial interests or personal relationships that could have appeared to influence the work reported in this paper.

Acknowledgments

We thank Dr. Claudia Squillaci and Dr. Claudia P. Anzola from the Servicio de Bioquímica in the Hospital Regional Diego Paroissien, Mendoza, Argentina, and Dr. Sandra M. Romano from the Instituto Coordinador de Ablación e Implantes Mendoza (InCAIMen), Mendoza, Argentina. for providing us with clinical samples of patients. We also thank Julieta Scelta, Adrian Fernandez, Tirso Sartor, Paula Lopez and Dra. Alfonsina Morales, from the Instituto de Histología y Embriología, Universidad Nacional de Cuyo (IHEM-CONICET-UNCUYO) for their excellent technical assistance. We also acknowledge Dr. Sebastian Real for the provision of NSG mice. This work was supported by funds from Departamento de Investigación, Ciencia y Técnica (Dicyt), Ministerio de Salud, Desarrollo Social y Deportes, Gobierno de Mendoza, Argentina (Proyecto Investigadores Mendocinos 2016) and from the Agencia Nacional de Promoción Científica y Tecnológica, Argentina (PICT 2013–2757) to PSR.

Supplementary materials

Supplementary material associated with this article can be found, in the online version, at doi:10.1016/j.crmicr.2022.100152.

References

Abegg, C.P., de Abreu, A.P., da Silva, J.L., de Araújo, S.M., Gomes, M.L., Ferreira, É.C., et al., 2017. Polymorphisms of blood forms and *in vitro* metacyclogenesis of Trypanosoma cruzi I, II, and IV. Exp. Parasitol. 176, 8–15.

Andrade, L.O., Machado, C.R.S., Chiari, E., Pena, S.D.J., Macedo, A.M., 1999. Differential tissue distribution of diverse clones of Trypanosoma cruzi in infected mice. Mol. Biochem. Parasitol. 100 (2), 163–172. May 25.

Arias-del-Angel, J.A., Santana-Solano, J., Santillán, M., Manning-Cela, R.G., 2020. Motility patterns of Trypanosoma cruzi trypomastigotes correlate with the efficiency of parasite invasion *in vitro*. Sci. Rep. 10 (1), 1–11, 10:1 [Internet]. 2020 Sep 28 [cited 2022 Apr 18]Available from: https://www.nature.com/articles/s41598-020-72604-4.

da S do Bahia, M.T., Andrade, IM de, Martins, T.A.F., Nascimento, Á.F., Diniz L de, F., Caldas, I.S., et al., 2012. Fexinidazole: a potential new drug candidate for chagas disease, Pollastri MP, editor PLoS Negl. Trop. Dis. 6 (11), e1870. Nov 1.

Brenière, S.F., Waleckx, E., Barnabé, C., 2016. Over six thousand trypanosoma cruzi strains classified into discrete typing units (DTUs): attempt at an inventory. Debrabant A, editor. PLOS Negl. Trop. Dis. [Internet] 10 (8), e0004792. Aug 29 [cited 2019 Nov 22]Available from: 10.1371/journal.pntd.0004792.

Campos, M.C.O., Leon, L.L., Taylor, M.C., Kelly, J.M., 2014a. Benznidazole-resistance in Trypanosoma cruzi: evidence that distinct mechanisms can act in concert. Mol. Biochem. Parasitol. 193 (1), 17–19.

Campos, M.C.O., Leon, L.L., Taylor, M.C., Kelly, J.M., 2014b. Benznidazole-resistance in Trypanosoma cruzi: evidence that distinct mechanisms can act in concert. Mol. Biochem. Parasitol. 193 (1), 17–19. Jan.

Casassa, A.F., Vanrell, M.C., Colombo, M.I., Gottlieb, R.A., Romano, P.S., 2019a. Autophagy plays a protective role against Trypanosoma cruzi infection in mice. Virulence 10 (1), 151–165. Jan 1.

Casassa, A.F., Vanrell, M.C., Colombo, M.I., Gottlieb, R.A., Romano, P.S., 2019b. Autophagy plays a protective role against Trypanosoma cruzi infection in mice. Virulence 10 (1), 151–165. Jan 1.

CDC - Chagas Disease - Biology [Internet]. [cited 2020 Aug 3]. Available from: https://www.cdc.gov/parasites/chagas/biology.html.

CDC - Chagas Disease - Epidemiology & Risk Factors [Internet]. [cited 2020 Aug 3]. Available from: https://www.cdc.gov/parasites/chagas/epi.html.

Chagas disease - PAHO/WHO | Pan American Health Organization [Internet]. [cited 2020 Aug 3]. Available from: https://www.paho.org/en/topics/chagas-disease.

Chuenkova, M.V., PereiraPerrin, M., 2009. Trypanosoma cruzi targets Akt in host cells as an intracellular antiapoptotic strategy. Sci. Signal. 2 (97). Nov 17.

Cortez C., Martins R.M., Alves R.M., Silva R.C., Bilches L.C., Macedo S., et al. Differential infectivity by the oral route of trypanosoma cruzi lineages derived from Y Strain. PLOS Negl. Trop. Dis. [Internet]. 2012 Oct [cited 2022 Apr 18];6(10):e1804.

Available from: https://journals.plos.org/plosntds/article?id=10.1371/journal.pntd.0001804.
Cosentino, R.O., Agüero, F., 2012. A simple strain typing assay for Trypanosoma cruzi: discrimination of major evolutionary lineages from a single amplification product. PLoS Neglected Tropical Diseases 6 (7).
Coura, J.R., De Castro, S.L., 2002. A critical review on chagas disease chemotherapy. Memorias do Instituto Oswaldo Cruz. Fundacao Oswaldo Cruz 97, 3–24.
Cura, C.I., Duffy, T., Lucero, R.H., Bisio, M., Péneau, J., Jimenez-Coello, M., et al., 2015. Multiplex real-time PCR assay using taqman probes for the identification of trypanosoma cruzi DTUs in biological and clinical samples. PLoS Negl. Trop. Dis. 9 (5). May 19.
De Diego, J.A., Penin, P., Del Rey, J., Mayer, R., Gamallo, C, 1991. A comparative pathological study of three strains of Trypanosoma cruzi in an experimental model. Histol. Histopathol. 6 (2), 199–206.
de Figueiredo Diniz, L., Mazzeti, A.L., Caldas, I.S., Ribeiro, I., Bahia, M.T., 2018. Outcome of E1224-Benznidazole combination treatment for infection with a multidrug-resistant trypanosoma cruzi strain in mice. Antimicrob. Agents Chemother. 62 (6). Jun 1.
Fernandes, M.C., Andrews, N.W., 2012. Host cell invasion by Trypanosoma cruzi: a unique strategy that promotes persistence [Internet]. FEMS Microbiol. Rev. 36, 734–747. FEMS Microbiol Rev[cited 2020 Aug 4]Available from: https://pubmed.ncbi.nlm.nih.gov/22339763/.
Filardi, L.S., Brener, Z., 1984. A rapid method for testing *in vivo* the susceptibility of different strains of Trypanosoma cruzi to active chemotherapeutic agents. Mem. Inst. Oswaldo Cruz 79 (2), 221–225.
Katsuno, K., Burrows, J.N., Duncan, K., van Huijsduijnen, R.H., Kaneko, T., Kita, K., et al., 2015. Hit and lead criteria in drug discovery for infectious diseases of the developing world. Nat. Rev. Drug Discov. [Internet] 14 (11), 751–758. Nov 1 [cited 2022 Apr 18]Available from: https://pubmed.ncbi.nlm.nih.gov/26435527/.
Lewinsohn, R., 1981. Carlos Chagas and the discovery of Chagas's disease (American Trypanosomiasis). J. R. Soc. Med. 74 (6), 451–455.
Macchiaverna, N.P., Enriquez, G.F., Buscaglia, C.A., Balouz, V., Gürtler, R.E., Cardinal, M.V., 2018. New human isolates of Trypanosoma cruzi confirm the predominance of hybrid lineages in domestic transmission cycle of the Argentinean Chaco. Infection Genetics and Evolution 66, 229–235. Dec 1.
Maffey, L., Cardinal, M.V., Ordóñez-Krasnowski, P.C., Lanati, L.A., Lauricella, M.A., Schijman, A.G., et al., 2012. Direct molecular identification of Trypanosoma cruzi Discrete Typing Units in domestic and peridomestic Triatoma infestans and Triatoma sordida from the Argentine Chaco. Parasitology 139 (12), 1570–1579. Oct 19.
Marcili, A., Lima, L., Cavazzana, M., Junqueira, A.C.V., Veludo, H.H., Maia Da Silva, F., et al., 2009. A new genotype of Trypanosoma cruzi associated with bats evidenced by phylogenetic analyses using SSU rDNA, cytochrome b and Histone H2B genes and genotyping based on ITS1 rDNA. Parasitology 136 (6), 641–655. May.
Martinez, S.J., Romano, P.S., Engman, D.M., 2020a. Precision health for chagas disease: integrating parasite and host factors to predict outcome of infection and response to therapy. Front. Cell Infect. Microbiol. 10 (May), 1–11.
Martinez, S.J., Romano, P.S., Engman, D.M., 2020b. Precision health for chagas disease: integrating parasite and host factors to predict outcome of infection and response to therapy. Front. Cell Infect. Microbiol. 10, 210. May 8.
Medina, L., Castillo, C., Liempi, A., Herbach, M., Cabrera, G., Valenzuela, L., et al., 2018. Differential infectivity of two Trypanosoma cruzi strains in placental cells and tissue. Acta Trop. 186, 35–40. Oct.
Melo, R.C., Brener, Z., 1978. Tissue tropism of different Trypanosoma cruzi strains. J. Parasitol. 64 (3), 475–482.
Menna-Barreto, R.F.S., 2019. Cell death pathways in pathogenic trypanosomatids: lessons of (over)kill. Cell Death Dis. [Internet] 10 (2). Feb 1 [cited 2022 Apr 18] Available from: https://pubmed.ncbi.nlm.nih.gov/30700697/.
Meymandi, S.K., Forsyth, C.J., Soverow, J., Hernandez, S., Sanchez, D., Montgomery, S. P., et al., 2017. Prevalence of Chagas disease in the Latin American-born population of Los Angeles. Clin. Infect. Dis. 64 (9), 1182–1188 [Internet][cited 2019 Nov 22] Available from: http://www.ncbi.nlm.nih.gov/pubmed/28329123.
Morilla, M.J., Montanari, J.A., Prieto, M.J., Lopez, M.O., Petray, P.B., Romero, E.L., 2004. Intravenous liposomal benznidazole as trypanocidal agent: increasing drug delivery to liver is not enough. Int. J. Pharm. 278 (2), 311–318. Jul 8.
Nunes, M.C.P., Dones, W., Morillo, C.A., Encina, J.J., Ribeiro, A.L., 2013. Chagas disease: an overview of clinical and epidemiological aspects. J. Am. Coll. Cardiol. 62, 767–776.
Osorio, L., Ríos, I., Gutiérrez, B., González, J., 2012. Virulence factors of Trypanosoma cruzi: who is who? Microbes and Infect. 14 (15), 1390–1402.
Paula M.N., Fabián G., Carlos Andrés B., Virginia B., Esteban R., Victoria M. New human isolates of Trypanosoma cruzi confirm the predominance of hybrid lineages in domestic transmission cycle of the Argentinean Chaco. 2018.
Penin P., Gamallo C., de Diego J.A. Biological comparison between three clones of trypanosoma cruzi and the strain of origin (Bolivia) with reference to Clonal Evolution Studies. Vol. 91, Memorias do Instituto Oswaldo Cruz. Fundacao Oswaldo Cruz; 1996. p. 285–91.
Pérez-Molina, J.A., Molina, I., 2018. Chagas Disease. The Lancet. Lancet Publishing Group, pp. 82–94. Vol. 391.
Quebrada Palacio, L.P., González, M.N., Hernandez-Vasquez, Y., Perrone, A.E., Parodi-Talice, A., Bua, J., et al., 2018a. Phenotypic diversity and drug susceptibility of Trypanosoma cruzi TcV clinical isolates. PLOS ONE [Internet] 13 (9), e0203462. Sep 1 [cited 2022 Apr 18]Available from: https://journals.plos.org/plosone/article?id=10.1371/journal.pone.0203462.
Quebrada Palacio, L.P., González, M.N., Hernandez-Vasquez, Y., Perrone, A.E., Parodi-Talice, A., Bua, J., et al., 2018b. Phenotypic diversity and drug susceptibility of Trypanosoma cruzi TcV clinical isolates. PLoS ONE 13 (9). Sep 1.
Rajão, M.A., Furtado, C., Alves, C.L., Passos-Silva, D.G., de Moura, M.B., Schamber-Reis, B.L., et al., 2014. Unveiling Benznidazole's mechanism of action through overexpression of DNA repair proteins in Trypanosoma cruzi. Environ. Mol. Mutagenesis [Internet] 55 (4), 309–321. May 1 [cited 2022 Apr 18]Available from: https://onlinelibrary.wiley.com/doi/full/10.1002/em.21839.
Recommendations from a satellite meeting. In: Memórias do Instituto Oswaldo Cruz. Fundação Oswaldo Cruz; 1999. p. 429–32.
Reynolds, E.S, 1963. The use of lead citrate at high pH as an electron-opaque stain in electron microscopy. J Cell Biol 17 (1), 208–212.
Romano P.S., Arboit M.A., Vázquez C.L., Colombo M.I. The autophagic pathway is a key component in the lysosomal dependent entry of Trypanosoma cruzi into the host cell. 104161/auto517160 [Internet]. 2009 Jan 1 [cited 2022 Apr 18];5(1):6–18. Available from: https://www.tandfonline.com/doi/abs/10.4161/auto.5.1.7160.
Spurr, A.R., 1969. A low-viscosity epoxy resin embedding medium for electron microscopy. J. Ultrasructure Res. 26 (1–2), 31–43.
Tyler, K.M., Engman, D.M., 2001. The life cycle of Trypanosoma cruzi revisited. Int. J. Parasitol. 472–481.
Vago, A.R., Andrade, L.O., Leite, A.A., d'Ávila Reis, D., Macedo, A.M., Adad, S.J., et al., 2000. Genetic characterization of Trypanosoma cruzi directly from tissues of patients with chronic chagas disease: differential distribution of genetic types into diverse organs. Am. J. Pathol. 156 (5), 1805–1809.
Vanrell, M.C., Losinno, A.D., Cueto, J.A., Balcazar, D., Fraccaroli, L.V., Carrillo, C., et al., 2017. The regulation of autophagy differentially affects Trypanosoma cruzi metacyclogenesis. PLoS Negl. Trop. Dis. 11 (11). Nov 1.
Velásquez, A.M.A., Francisco, A.I., Kohatsu, A.A.N., Silva FA de, J., Rodrigues, D.F., Teixeira, R.G., da, S., et al., 2014. Synthesis and tripanocidal activity of ferrocenyl and benzyl diamines against Trypanosoma brucei and Trypanosoma cruzi. Bioorg Med. Chem. Lett. 24 (7), 1707–1710. Apr 1.
Velazquez, E., Meeks, B., Bonilla, L., Rassi, A., Bonilla, R., Lazdins, J., et al., 2015. Randomized trial of Benznidazole for chronic Chagas' cardiomyopathy. N. Engl. J. Med. 373 (14), 1295–1306. Oct 30.
Viotti, R., Vigliano, C., Lococo, B., Alvarez, M.G., Petti, M., Bertocchi, G., et al., 2009. Side effects of benznidazole as treatment in chronic Chagas disease: fears and realities. Expert Rev. Anti Infect. Ther. 7 (2), 157–163. Mar 10.
Virreira, M., Alonso-Vega, C., Solano, M., Jijena, J., Brutus, L., Bustamante, Z., et al., 2006. Congenital chagas disease in bolivia is not associated with dna polymorphism of trypanosoma cruzi. Am. J. Trop. Med. Hyg. 75 (5), 871–879 [Internet]Nov 1 [cited 2022 Apr 18]Available from: https://www.ajtmh.org/view/journals/tpmd/75/5/article-p871.xml.
Zingales, B., Andrade, S., Briones, M., Campbell, D., Chiari, E., Fernandes, O., et al., 2009. A new consensus for Trypanosoma cruzi intraspecific nomenclature: second revision meeting recommends TcI to TcVI. Memórias do Instituto Oswaldo Cruz 104 (7), 1051–1054. Nov.
Zingales, B., Miles, M.A., Campbell, D.A., Tibayrenc, M., Macedo, A.M., Teixeira, M.M. G., et al., 2012. The revised Trypanosoma cruzi subspecific nomenclature: rationale, epidemiological relevance and research applications. Infect., Genetics and Evolution. Infect. Genet. Evol. 12, 240–253.